Analytica Chimica Acta 1140 (2020) 111–121

Contents lists available at ScienceDirect

Analytica Chimica Acta

journal homepage: www.elsevier.com/locate/aca

Highly fluorescent hematoporphyrin modified graphene oxide for selective detection of copper ions in aqueous solutions

Fathi S. Awad [a, b, *], Khaled M. AbouZied [a], Ayyob M. Bakry [a, c], Weam M. Abou El-Maaty [b], Ahmad M. El-Wakil [b], M. Samy El-Shall [a, **]

[a] Department of Chemistry, Virginia Commonwealth University, Richmond, VA, 23284, USA
[b] Chemistry Department, Faculty of Science 35516, Mansoura University, Mansoura, Egypt
[c] Department of Chemistry, Faculty of Science, Jazan University, Jazan, 45142, Saudi Arabia

HIGHLIGHTS

- Hematoporphyrin modified graphene oxide (HP-GO) was synthesized as an efficient optical fluorescence sensor.
- The HP-GO was used as a very effective fluorescent probe for sensitive and selective detection of Cu^{2+}.
- The HP-GO sensor displayed attractive long term fluorescence stability (> 21 days) in water.
- The HP-GO sensor has been applied successfully for real water sample analysis.

GRAPHICAL ABSTRACT

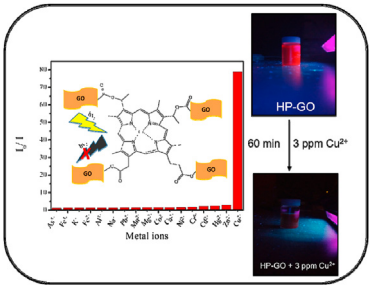

ARTICLE INFO

Article history:
Received 16 August 2020
Received in revised form
4 October 2020
Accepted 8 October 2020
Available online 14 October 2020

Keywords:
Graphene oxide
Modification
Hematoporphyrin
Detection
Fluorescence
Sensor
Esterification
Copper

ABSTRACT

Here, a highly sensitive and selective copper ion (Cu^{2+}) fluorescence sensor is reported. The Hematoporphyrin functionalized Graphene Oxide (HP-GO) fluorescence sensor were synthesized via esterification reaction between Graphene Oxide and Hematoporphyrin (HP). The HP-GO sensor was fully characterized by Fourier Transform Infrared Spectroscopy (FTIR), X-ray diffraction (XRD), Scanning Electrom Microscopy (SEM), UV–Vis spectroscopy, Transmission Electron Microscopy (TEM), Fluor meter spectroscopy, X-Ray photoelectron spectroscopy(XPS), and Raman spectroscopy measurements. The HP-GO sensor advertised two linear regions over the range of 0–1.18 × 10^3 nM and 3.93 × 10^3 to 47.27 nM of copper (II) with detection limit of 54 nM in the aqueous solution. The selectivity of HP-GO for Cu^{2+} is much higher than that of other metal ions due to the presence of aza macrocyclic ring on the surface of HP-GO which has a high binding affinity with Cu^{2+}. Additionally, the HP-GO shows wide pH viable range (pH 6–10). The effect of other metal ions on the fluorescence intensity of the HP-GO was also studied and other metal ions show a low interference response in the detection of Cu^{2+}. HP-GO sensor manifests advantages of high reproducibility (The quenched fluorescence of HP/GO-Cu can be recovered by EDTA), attractive long term fluorescence stability (>21 days) in water, also remarkable selectivity regarding number of metal ions (Na^+, K^+, Ca^{2+}, Fe^{3+}, Fe^{2+}, Al^{3+}, Pb^{2+}, Mn^{2+}, Mg^{2+}, Co^{2+}, Ni^{2+}, Cr^{6+}, Cd^{2+}, Hg^{2+}, and

* Corresponding author. Chemistry Department, Faculty of Science 35516, Mansoura University, Mansoura, Egypt.
** Corresponding author. Department of Chemistry, Virginia Commonwealth University, Richmond, VA, 23284, USA.
E-mail addresses: fathyawad949@yahoo.com (F.S. Awad), mselshal@vcu.edu (M.S. El-Shall).

https://doi.org/10.1016/j.aca.2020.10.016

Zn^{2+}), low toxicity and can detect Cu^{2+} in real water samples which acquire well for its promising in environmental applications.

1. Introduction

The research on copper (II) (Cu^{2+}) has gained a great consideration in recent years because of its vital role in various metabolism and biological processes for all organisms [1–3]. Copper is considered one of the most abundant transition metal in life after iron and zinc [4,5], Cu^{2+} is also extremely important for the electron transfer processes of different biological processes in the human body [6–8]. The enzyme activity can be effected by the shortage of Cu^{2+} leading to several neurological problems in the body, whereas the increase of copper ions is associated to the deterioration of livers, kidneys, lethargy, increased blood pressure, vomiting, neurotoxicity, acute hemolytic anemia, respiratory rates, and neurodegenerative diseases such as Alzheimer's, Parkinson's, and prion diseases [3,9–13]. According to WHO (World Health Organization) the maximum permissible level of Cu^{2+} ion concentration in drinking water is 2 mg L^{-1} while allowable levels of Cu^{2+} according to US EPA (Environmental Protection Agency) is 1.3 mg L^{-1} [14,15]. Thus, developing efficient methods having highly selective and sensitive determination of Copper (II) are of considerable interest to the environmental and scientific communities [3]. Many analytical methods have been applied for the accurate determination of Cu^{2+} ions, Chemiluminescence [16], Inductively-Coupled Plasma Mass Spectrometry (ICPMS) [17], Atomic Absorption/Emission Spectroscopy (AAS/AES) [18,19], Electrochemical methods [20,21] and Colorimetric methods [22]. Among these, Fluorescence spectrometry has gained great concern, due to its advantages of high sensitivity and rapid response [23,24]. Fluorescent chemo sensors are extensively used to detect ions in solution, owing to their advantages of high sensitivity, simplicity and selectivity. Several new fluorescent chemo sensors have been synthesized for detection of Cu^{2+} such as fluorescent carbon dots [25], amidine/Schiff base modified polyacrylonitrile [11], graphitic carbon nitride [26], and cyclam-functionalized carbon dots [27].

Porphyrins are heterocyclic macro cycles and as highly conjugated planar systems demonstrate the intense absorption and emission of light, which can be modulated by peripheral substitutes [28,29]. Porphyrins are considered as strong macro cyclic ligands and have been utilized as highly sensitive probe molecules in several chemical sensors for the accurate detection of metal ions [28,30,31]. The high sensitivity of porphyrins can be attributed to the pairs of electrons of nitrogen atoms in the porphyrin ring which have high affinity to coordinate with the metal ions and therefore highly stable complexes are formed [32,33]. The UV–vis spectra of porphyrins shows a characteristic weak absorption peaks in the range of 500–700 nm and a strong absorption peak in the range of 400–420 nm. These peaks are due to $\pi-\pi^*$ electron transition of porphyrin unsaturated ligands [28]. Subsequently, porphyrins are a good choice to use as a receptor in the optical sensors. A proper substrate should have proper functional groups to chemically bonded to the receptor.

Graphene oxide (GO) is the oxidized form of graphene (a two-dimensional sheet of sp^2 hybridized carbon atoms), which has recently attracted significant attention due to many outstanding properties (e.g. large surface area, high flexibility, inexpensive and readily obtained, high mechanical strength, excellent physicochemical stability, and unique layered structure) [34–37]. Most importantly, graphene oxide nanosheets with hydroxyl, carboxyl, and epoxy functional groups are able to chemically bond to porphyrins. Although graphene has huge potential for sensor applications, there are only a few reports published on using modified graphene as sensors for chemical detection of metal ions in the aqueous media.

Here, we describe a simple and efficient fluorescence sensor for detecting Cu^{2+}. For this sensor, Hematoporphyrin (an effective ligand for Cu^{2+}) is used for the chemical modification of the graphene oxide sheets. The Hematoporphyrin/Graphene oxide (HP-GO) sensor was prepared by esterification reaction between graphene oxide nanosheets (GO) and Hematoporphyrin (HP) in the presence of sulfuric acid. Because $Cu^{2+}$is hard acid and Hematoporphyrin is aza macrocyclic ligand (hard base) leads to the formation of stable complex so HP-GO is highly effective to detect Cu^{2+} ions [38]. The structure and morphology of HP-GO was confirmed by Raman spectra measurements, Fourier transform infrared spectroscopy (FT-IR), Scanning Electron Microscopy (SEM), X-ray diffraction analysis (XRD), UV–Vis spectra, X-ray photoelectron spectroscopy (XPS), TEM using the Jeol JEM-1230 microscope, and Fluorescence Spectroscopy. To improve the sensor response, various experimental parameters such as contact time, pH, selectivity and effect of other metal ions on the fluorescence quenching of HP-GO. In addition, it's practical application in detecting Cu^{2+} in real water samples (tap, and river water). The recovery of fluorescence intensity of HP-GO was also studied.

2. Experimental section

2.1. Materials

Graphite powder of high purity 99.9999% was used. The oxidizing mixture was concentrated H_2SO4 98%, and$KMnO_4$99%. Sodium Nitrate used was 99%. Ethylenediaminetetraacetic acid (EDTA) ≥ 98%. The H_2O_2 used was of 30% concentration. Hematoporphyrin ≥45%. All reagents were purchased from sigma Aldrich and used without further purification. Stock solutions of ions at various concentrations were prepared from $CuCl_2\cdot 2H_2O$, $Cd(NO_3)_2$, $HgCl_2$, $Ni(NO_3)_2\cdot 6H_2O$, $Pb(NO_3)_2$, $Mn(NO_3)_2$, $K_2Cr_2O_7$, KH_2AsO_4, $Zn(NO_3)_2\cdot 6H_2O$, NaCl, KCl, $CaCl_2$, and $Al(NO_3)_2$ were used as sources for Cu^{2+}, Cd^{2+}, Hg^{2+}, Ni^{2+}, Pb^{2+}, Mn^{2+}, Cr^{6+}, As^{5+}, Zn^{2+}, Na^+, K^+, Ca^{2+}, and Al^{3+} respectively. Metal ions of lower concentrations were prepared by further dilution using phosphate buffer, pH 8. Phosphate buffer solution (0.01 M) were prepared from sodium NaH_2PO_4/NaOH. Deionized (DI) water was used throughout these experiments.

2.2. Instruments

Fourier transform infrared (FT-IR) spectrum were recorded on a Nicolet-Nexus 670 FTIR Spectrometer (4 cm^{-1} resolution and 32 scan) Diamond Attenuated Total Reflectance (DATR) and a measuring range 400–4000 cm^{-1}, X-ray diffraction patterns were recorded in the 2θ range of 5–40 with a scanning speed of 2° in 2θ/min using an X'Pert Philips Materials Research Diffractometer. UV-2450 UV–Visible Spectrophotometer reequipped witha10-mmquartzcell, where the light path length was 1 cm. X-ray Photoelectron Spectroscopy (XPS) was performed on an XPS system (Thermo Fisher ESCAlab 250). The

morphology and structure of GO and modified GO were investigated by SEM (Hitachi SU-70 FE-SEM). Raman Spectra were obtained from Thermo Scientific DXR Smart Raman (532 nm) for GO before and after laser irradiation. Varian-Cary Eclipse Fluorescence Spectrometer.

2.3. Preparations of hematoporphyrin functionalized GO (HP-GO)

GO was prepared via the improved Hummer method [39,40] the improved Hummer method a mixture of graphite flakes (4.5 g) and potassium permanganate (27.0 g) was added to a mixture of concentrated H_3PO_4/H_2SO_4 (60:540 mL) producing a slight exotherm to 35–40 °C and maintained below 30 °C using ice bath. The reaction was then stirred and heated for 12 h at 50 °C. The mixture was cooled to room temperature and poured onto ice (600 mL) with 30% H_2O_2 (4.5 mL).The mixture was then filtered, and washed in succession with 30% HNO_3 (200 mL),H_2O (200 mL), and (2%) ethanol (200 mL); for each wash. The final product was vacuum dried at 60 °C for 12 h, obtaining 7.5 g of GO. To preapare HP-GO, 100 mg of GO, was dispersed well in 100 mL DI water, and the mixture was ultra-sounded for 1 h to give a clear solution. Next, 30 mg of Hematoporphyrin dissolved well in 100 mL acidified DI water was added to the GO solution followed by adding 1 mL concentrated Sulfuric acid to adjust pH to 1.5 and refluxed at 80°C for 7 h. The product was separated by centrifugation, washed with DI water several times until the pH of the supernatant become steady at about (pH = 6) and dried in oven at 70 °C for 10 h. The general steps for the preparation of hematoporphyrin modified graphene oxide is shown in Scheme 1.

2.4. Fluorescence sensing experiments

The effect of pH on the fluorescence intensity of HP-GO was recorded by varying solution pH (2–10) by adding few drops of 0.01 M HCl and 0.01 M NaOH solution. The intensity of fluorescence spectra was recorded using Varian-Cary Eclipse Fluorescence Spectrometer using an excitation wavelength of 390 nm and excitation and emission slit widths of 10 nm at room temperature.

2.5. Fluorescence detection of Cu^{2+}

The fluorescence sensing of Cu^{2+} was conducted in phosphate buffer solution (0.01 M, pH 8) at room temperature. In a typical run, 0.25 mL of HP-GO (10 mg L^{-1}) was added into 0.75 mL phosphate buffer, followed by the addition of a calculated amount of Cu^{2+} ions. The mixed solution was diluted to 2 mL by distilled water. The fluorescence quenching spectra were measured at room temperature at different times (1, 2, 3, 4, 5, 6, 7, 8, 13, 15, 18, 20, 27, 30, 35, 40, 45, 50, 55, and 60 min) using Varian-Cary Eclipse Fluorescence Spectrometer, using an excitation wavelength of 390 nm and excitation and emission slit widths of 10 nm.

2.6. Selectivity measurements of metal ions

As described before in the detection of copper, 0.25 mL of HP-GO (10 mg L^{-1}) was added into 0.75 mL phosphate buffer, followed by the addition of 0.6 mL (10 mg L^{-1}) of different metal ions Na^{+}, K^{+}, Ca^{2+}, Mn^{2+}, Co^{2+}, Fe^{2+}, Fe^{3+}, Zn^{2+}, Al^{3+}, Cr^{6+}, As^{5+}, Cd^{2+}, Zn^{2+}, Pb^{2+}, Hg^{2+} and Cu^{2+} solution. The mixed solution was diluted to

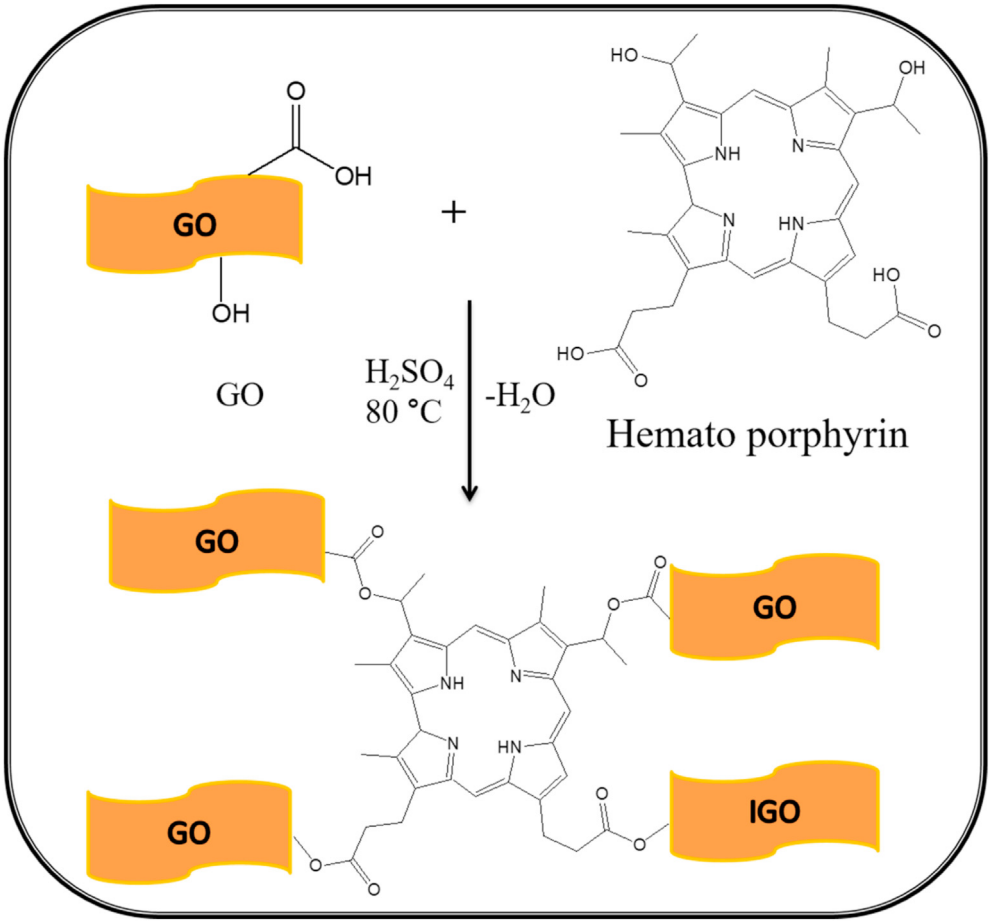

Scheme 1. General procedure for the preparation of hematoporphyrin modified Graphene oxide.

2 mL by distilled water. The fluorescence quenching spectra of the mixture solution was recorded.

2.7. Detection of Cu^{2+} ions in real water samples

In order to evaluate the HP-GO as sensor for Cu^{2+} in real sample, tap water and James River water were chosen as real sample. The river water, which was obtained from James river in Richmond, Virginia, USA., were centrifuged at 90,000 rpm for 10 min to remove solid impurities followed by filtration using filter paper. Then, the water sample was used in preparation of Cu^{2+} ion solution that will be added to the sensing system and the fluorescence spectra were recorded.

2.8. Detection limit

Is the lowest concentration of copper that can be detected using HP-GO sensor and can be determined by the fluorescence titration. The intensity of HP-GO emission without any Cu^{2+} and with Cu^{2+} was measured 5 times to measure the S/N ratio. The detection limit can be calculated by the following equation: detection limit = 3σ/S, where S is the slope between fluorescence intensity against Cu2+ concentration, and σ is the standard deviation of the blank measurements.

3. Results and DISCUSSION

3.1. Characterization of Graphene Oxide and Hematoporphyrin functionalized graphene oxide

The GO and HP-GO that were prepared were characterized by FTIR, XRD and Raman spectra analysis as shown in Fig. 1. These results confirmed that GO and HP-GO were synthesized successfully.

Fig. 1(A) shows the FTIR spectra of GO, and HP-GO. The broad absorption peak at 3350 cm^{-1} was attributed to O–H stretching vibrations. The peak at 1735 cm^{-1} was attributed to C=O stretch vibrations in the carboxylic groups of GO [41]. The FTIR spectra of HP-GO showed a characteristic new band at 1693 cm^{-1} which can be related to the bending vibrations of C=N, or the C=O stretching vibration of COO ester. New peak at 1577 cm^{-1} attributed to the C=C vibrations of porphyrins [28]. This indicated that the free OH groups in GO reacted with COOH groups in Hematoporphyrin to form ester bonds in presence of sulfuric acid. The peaks at 1420 cm^{-1} corresponds to the C–N bond, and the peak sat 1250, 1050, and 830 cm^{-1} refer to the C–OH stretching, symmetric, and a symmetric stretching vibration in epoxy groups, respectively.

The XRD pattern of GO and HP-GO are shown in Fig. 1B.The XRD pattern of GO displayed a sharp peak at about 10.55° with interlayer distance of 0.8 nm which was attributed to the oxygen-containing groups on the graphene sheets introduced due to oxidation of graphite. This makes the individual GO sheets thicker [34]. The XRD pattern of HP-GO displayed a new broad peak at $2\theta = 7.1^{\circ}$ with a longer inter layer spacing of graphene due to the chemical grafting of hematoporphyrin onto the GO sheets which could result in larger spacing between the exfoliated layers due to the bulky size of the porphyrin ring.

Fig. 1C shows the Raman spectra of GO, and HP-GO. It exhibited two characteristic peaks of D-band and G-band at around 1356, and 1605 cm^{-1}. The D band is due to the disorder in the graphitic structure. The intensity ratio of the D and G band (ID/IG) corresponds to the number and size of the sp^2 clusters of the material. The ID/IG of HP-GO shows (1.03) slightly enhanced after modification with Hematoporphyrin with that of GO (0.95) representing the improvement of disordered graphene sheets and increase in sp^2 clusters and confirming that the Hematoporphyrin are covalently attached to the graphene oxide sheets [42].

Fig. 2 displays SEM images of GO (A) and HP-GO (B), and the corresponding TEM images are presented in Fig. 2 (C) and 2(D), respectively. As compared to that of GO, SEM and TEM images of HP-GO reveals that the GO sheets become more thick and rough surfaces, as well as a lower transparence, this may be attributed to the reaction between the oxygen containing functional groups of GO and Hematoporphyrin molecules. This gives a good indication of the successful incorporation and grafting of HP molecules on the graphene sheets which guarantees the subsequent satisfactory fluorescence sensing application.

The grafting of HP molecules onto the surface of graphene oxide nanosheets was confirmed by x-ray photon spectroscopy shown in Fig. 3. In the wide scan XPS spectra shown in Fig. 3(A) and 3(B), The intensity of the peak corresponding to C 1s and O 1s decreased significantly from GO and HP-GO. Additionally, The HP-GO sample also clearly shows high intense N 1s peak. These observations confirmed that HP-GO was successfully formed, and HP molecules was simultaneously grafted on the surface of GO through esterification reaction between the free OH groups of GO and the COOH groups of HP in covalently hybrid structured (HP-GO). The C 1s high resolution (Fig. 3A) related to the GO was deconvoluted to three peaks with binding energies about 284.7 (C in C–H, C=C), 288.3 (C in C=O), and 286.2(C in C–O) [43]. The high resolution spectra of C

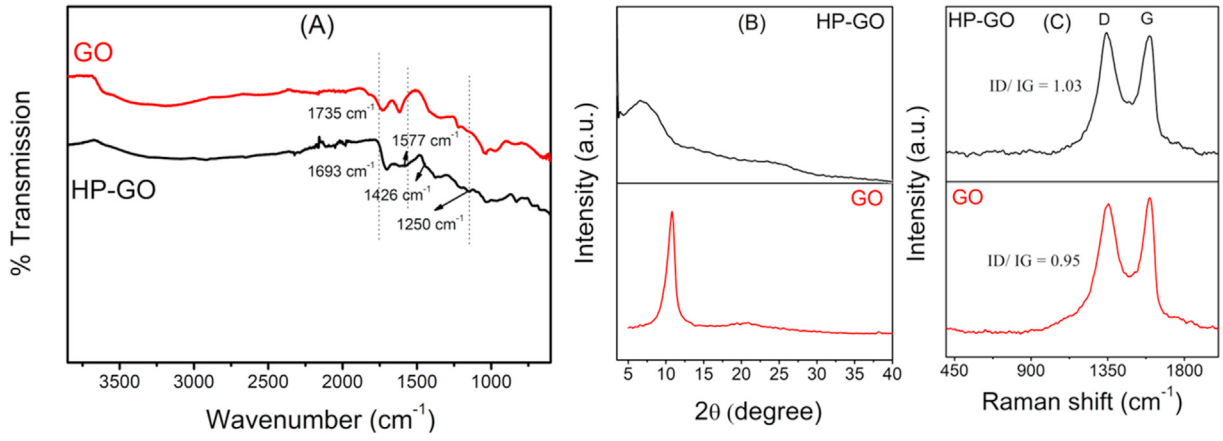

Fig. 1. (A) FTIR spectra of GO and HP-GO. (B) XRD patterns of GO, and HP-GO. (C) Raman spectra of GO, and HP-GO.

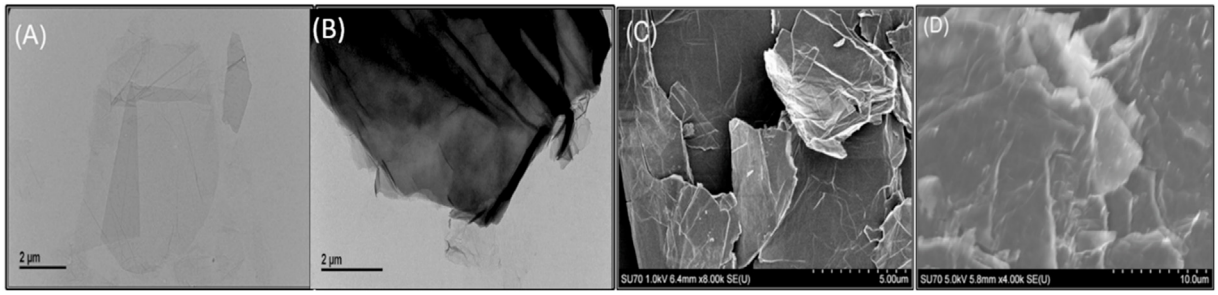

Fig. 2. TEM and SEM images of GO (A, C), and HP-GO (B, D).

1s (Fig. 4C) related to HP-GO was deconvoluted to four peaks with bending energies about 284.8 (C in C═C, C–H, C–C), 287.6 (C in C–N, C═N), 286.6 (C in C═N, C–O), and 288.8 (C in O–C═O). So the chemical modification with HP was confirmed by the peaks at 286.6, and 287.6 for C═N, and C–N) [44]. The high resolution of N 1s peak (Fig. 4F) related to HP-GO can be deconvoluted into two peaks 399.9 (N in pyrrole NH-, C–N) and 397.7 (N in pyrrole N, C═N). The high-resolution oxygen O 1s peak related to HP-GO can be deconvoluted to three peaks at 533, 529.6, and 531.8 related to O in O═C–O, O–H, and C═O, respectively).

Fig. 4 presents the UV–Vis absorption spectra of Hematoporphyrin ligand, GO, and HP-GO. For Hematoporphyrin Ligand, The porphyrins shows two characteristic bands in UV–Vis spectrum named Q band in the range 550–593 nm and Soret band in the range of 380–450 nm, which related to the π-π* electron transfer [28]. Fig. 4 shows two absorption peaks at 552 and 594 nm and a strong peak at 391 nm. For GO, The UV–Vis spectrum showed two bands: a shoulder at 304 nm assigned to n-π* transition of C═O, and C–O and a maximum between 233 nm, which can be related to the π-π* absorption of aromatic C═C bonds [45]. For HP-GO, Fig. 4 shows the presence of GO peak around 233 nm and the characteristic peaks of Hematoporphyrin with a red shift of the π-π* Soret band from (345–414) to (351–445).This shift suggests that the energy gap between the ground and excited orbitals of Hematoporphyrin in HP-GO is decreased due to the interaction between GO and HP [46]. In addition, the appearance of the peaks at 391 and 552 nm confirmed the presences of HP and GO in HP-GO.

3.1.1. *Absorbance and emission spectra of HP-GO*

The absorption spectrum of HP-GO in water solution is shown in Fig. 4. There is absorption peak existed at 390 nm represented a π-π* transition of the C═N group in the porphyrin ring. The fluorescence emission spectra and excitation of HP-GO are shown Fig. 5. We further analyzed the excitation dependent emission of the HP-GO by changing the excitation wavelength from (370–420 nm) (Fig. S2 (Supporting Information)). The maximum emission intensity of HP-GO was achieved at 614, and 676 nm ($\lambda_{max} = 390$ nm), which is the optimal excitation wavelength for the sensing experiments.

3.2. *Fluorescence sensing of Cu^{2+} using HP-GO*

Investigation of pH **dependence and long-term photo stability of HP-GO sensor.** It is known that the wide pH viable range is important for sensors in biological and environmental applications. The effect of pH on the HP-GO sensor is shown in Fig. 6. It can be noted that pH value from pH 6 to pH 10 have a negligible influence on the fluorescence intensity of HP-GO sensor but decreased in the

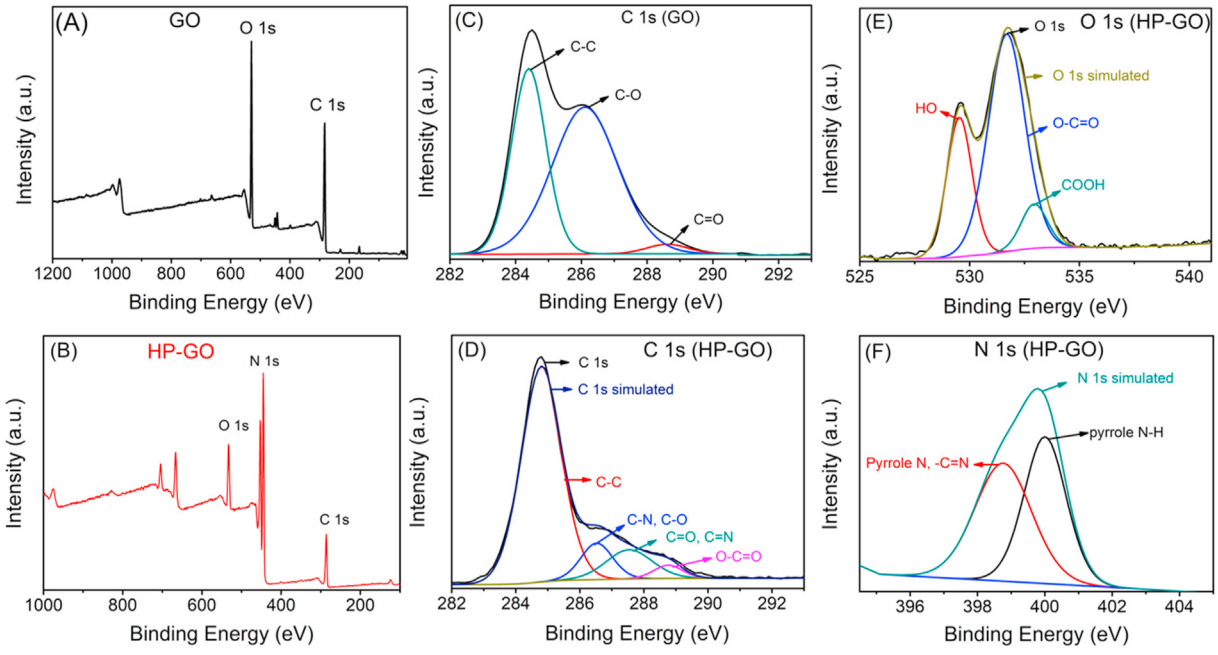

Fig. 3. XPS survey spectra of GO (A) and HP-GO (B), and XPS high resolution spectra of C1s in GO (C), C1s in HP-GO (D), O 1s in HP-GO (E) and N 1s in HP-GO (F).

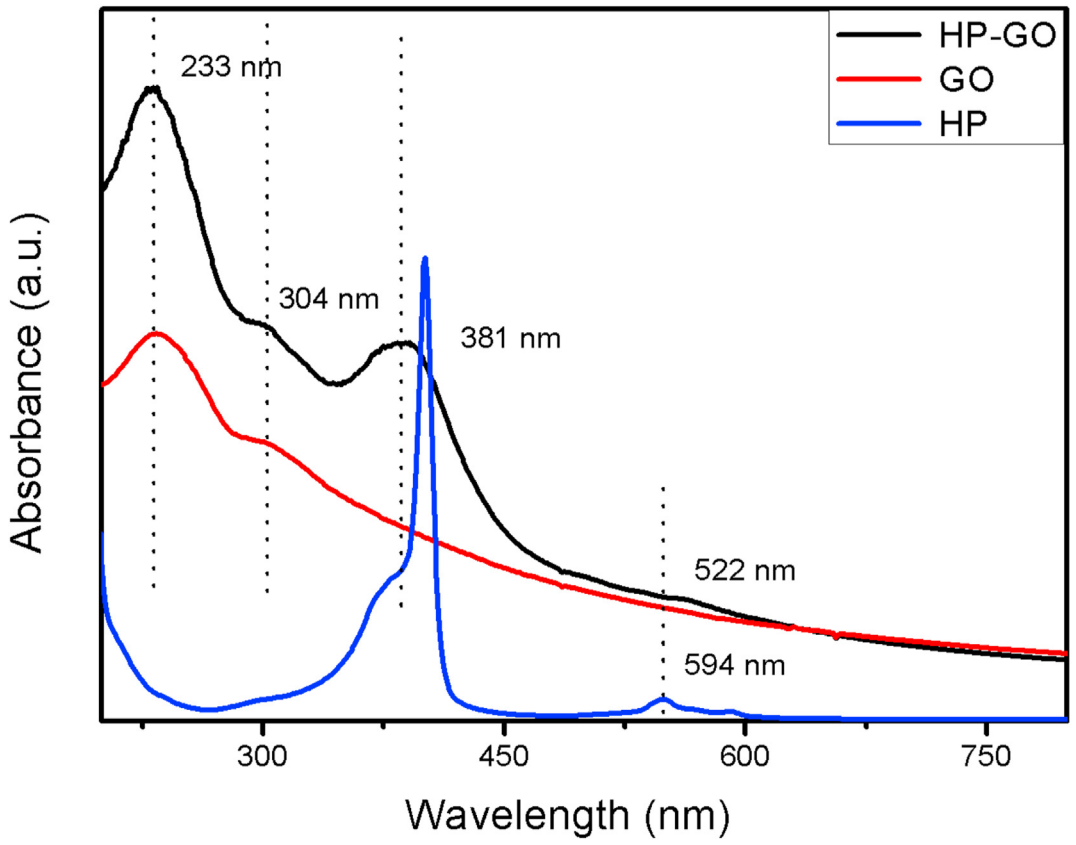

Fig. 4. UV–Vis spectra of GO and HP-GO.

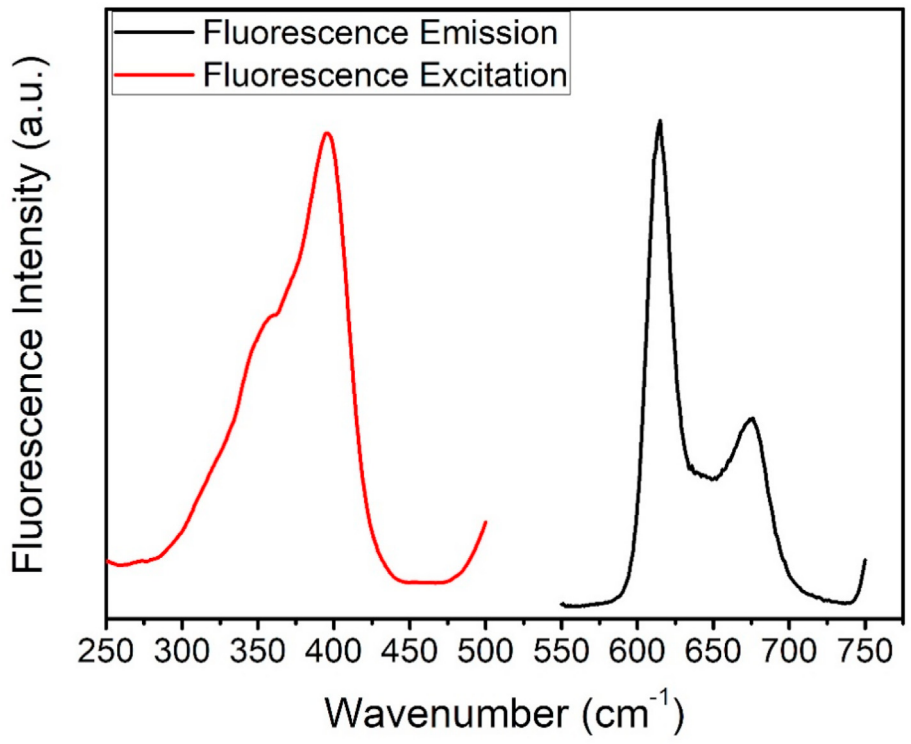

Fig. 5. Fluorescence spectra of HP-GO.

pH range of 2–5, so HP-GO can be used as sensor in a wide pH range. Also, the long-term stability of the HP-GO sensor was investigated. The HP-GO dispersion was stored in a glass vial and kept in dark under room temperature. Although it stored for more

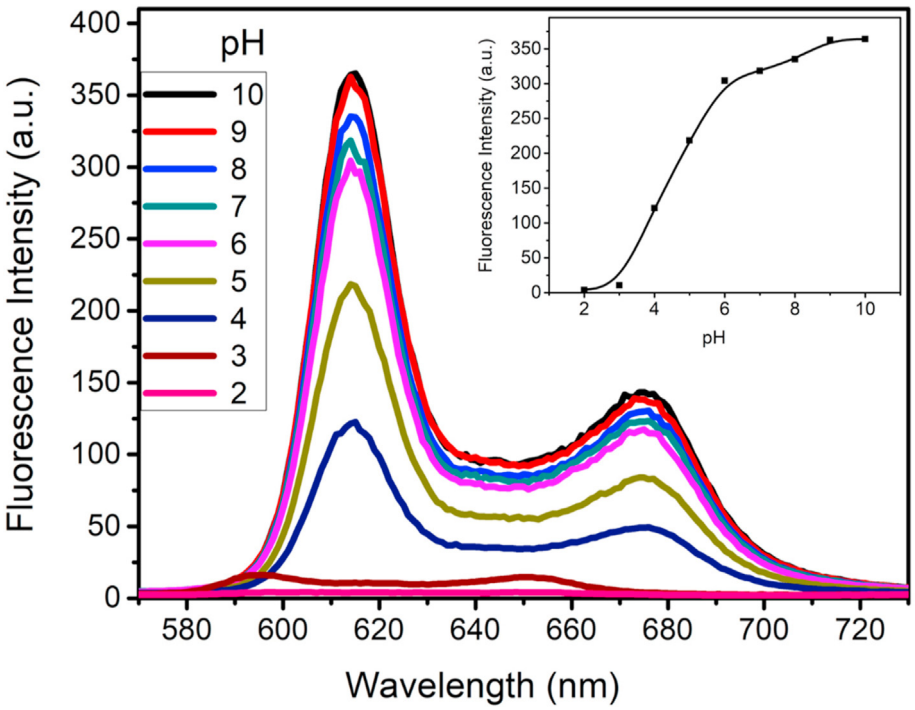

Fig. 6. The fluorescence emission spectra of HP-GO at different pH values, HP-GO = (10 mg L^{-1}), reaction time = (60 min), and excitation at 390 nm).

than 21 days, the intensity of HP-GO has a little bit change not more than 5%.

To identify the ability of HP-GO as sensor for Cu^{2+} detection. Figures (7) and (S3 (Supporting Information)) show that the fluorescence intensity of HP-GO decreased clearly on the introduction of Cu^{2+} ion in pH 8 using phosphate buffer, suggesting that Cu^{2+} can effectively quench the fluorescence of HP-GO nanosheets. Because Cu^{2+} is a hard acid and porphyrin is aza macrocyclic ligand (hard base) leads to the formation of stable complex and leads to electron transfer from HP-GO to the complexed Cu^{2+} leading to fluorescence quenching [38]. For sensitivity study, various concentrations of Cu^{2+} in the range of 0–3.5 ppm were carried out. Fig. 7 revealed that the fluorescence intensity of HP-GO at 614, and 676 nm (λ_{max} 390 nm) gradually decreased with increased Cu^{2+} till complete quenching at 3 ppm Cu^{2+} indicating that all co-ordination points on HP-GO nanosheets reacted with Cu^{2+}. Fig. 7 inset reveals the dependence of I/I_0 on the concentration of Cu^{2+} ions and a linear relationship between the concentration of copper ions and the emission intensities ($R^2 = 0.998$), where I and I_0 are the fluorescence intensities in the presence and absence of Cu^{2+}, respectively. The detection limit is evaluated to be 54 nM, suggesting that the HP-GO is suitable as sensitive detection probe for copper ions. It should be noted that this detection limit is sigficantly lower than the maximum allowable concentration of Cu^{2+} in drinking water (2 mg L^{-1} or 1.3 mg/L corresponding to 31.5 μM or 20.5 μM, respectively [14,15]. Compared with reported sensor in literature, the prepared HP-GO sensor has a wider linear range and good linear relation, which indicating that it is considered as a promising sensor for detection of Cu^{2+} in water samples. Recovery of Fluorescence intensity of HP-GO, Ethylenediaminetetraacetic acid was introduced into the solution containing Cu^{2+} ions and HP-GO as shown in Fig. S4 (Supporting Information). EDTA can coordinate with Cu^{2+} ions and the solution becomes free from metal ions [47]. The quenched fluorescence of HP-GO was recovered into strong fluorescence by EDTA treatment.

The effect of time on the fluorescence quenching of a HP-GO-Cu^{2+} solution was investigated. Figs. S5 and S6 (Supporting Information) showed that the fluorescence quenching enhanced with increased reaction time between Cu^{2+} and HP-GO. This is mainly due to the driving force making transfer of metal ions to the surface of HP-GO sheets and the availability of the co ordination points on the surface of HP-GO. Figs. S5 and S6 (Supporting Information) revealed that after 60 min, there is no significant change in the fluorescence intensity indicating that all co ordination points on HP-GO reacted with Cu^{2+} ions.

Selectivity is a very important parameter to estimate the capability of HP-GO as sensor for Cu^{2+} ions. To investigate the selectivity of this sensor, we recorded the change in the fluorescence intensity in the presence of representative metal ions under the same condition. As shown in Figs. 8 and S7 (Supporting Information), and the fluorescence of HP-GO was only quenched by the addition of copper ions (about 100% quenching up on addition 47 μM Cu^{2+} in phosphate buffer pH 8), while no significant quenching effect was observed with other metal ions (Hg^{2+}, As^{5+}, Cr^{6+}, Na^{+}, Ca^{2+}, K^{+}, Mg^{2+}, Fe^{2+}, Fe^{3+}, Pb^{2+}, Co^{2+}, Zn^{2+}, Al^{3+}, $Mn^{2+}$and Cd^{2+}). In general, copper ions have high tendency to coordinate with the porphyrin ring on HP-GO due to the unshared electrons of the nitrogen atoms in the porphyrin ring. Because of its paramagnetic property and unfilled d shell, only copper ion could strongly quench the fluorescence intensity of HP-GO through electron transfer processes [47–49].

The effect of interfering metal ions on the fluorescence intensity in copper ion detection using HP-GO was investigated Fig. 9, and we found that the emission intensity of the HP-GO to copper ions was almost unchanged in the presence of other metal ions, which indicate that copper ions have higher binding ability with porphyrin ring on the surface of HP-GO than other metal ions. The binding ability of HP-GO with various metal ions (Hg^{2+}, As^{5+}, Cr^{6+}, Na^{+}, Ca^{2+}, K^{+}, Mg^{2+}, Fe^{2+}, Fe^{3+}, Pb^{2+}, Co^{2+}, Zn^{2+}, Al^{3+}, Mn^{2+} and Cd^{2+}) showed a selective response toward Cu^{2+} ions. As shown in Fig. 9, the addition of Cu^{2+} resulted in a significant change indicating that the HP-GO has higher binding affinity towards Cu^{2+} than other metal ions. All these results demonstrate that the HP-GO is highly selective for copper ion detection.

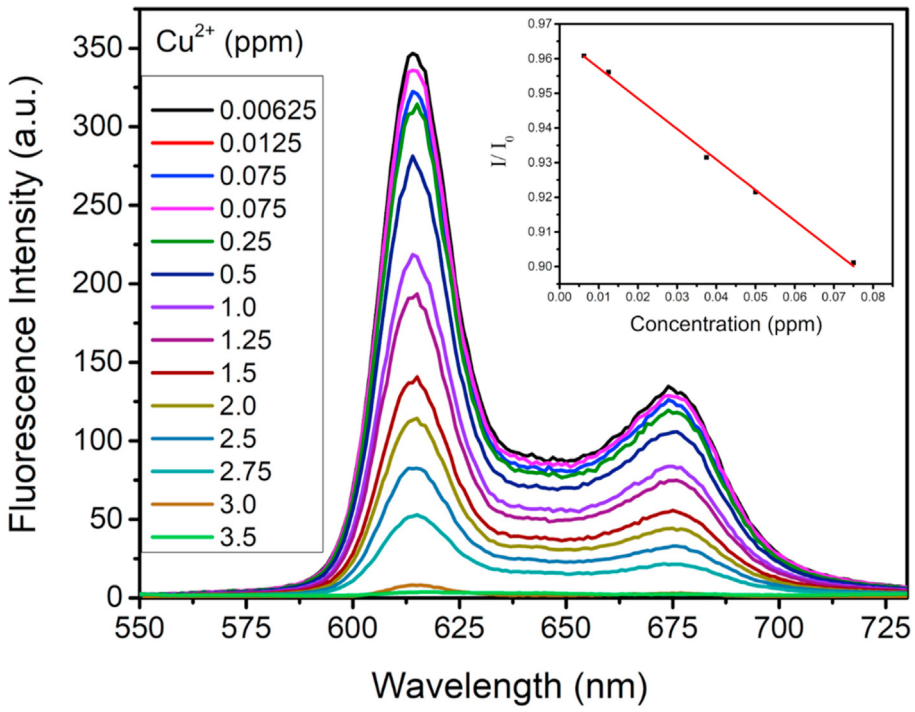

Fig. 7. Fluorescence emission spectra of HP-GO in the presence of Cu^{2+} at different concentrations (0–3.5 ppm), in 0.01 M phosphate buffer (pH = 8.2), HP-GO = (10 mg L^{-1}), reaction time = (60 min), and excitation at 390 nm).

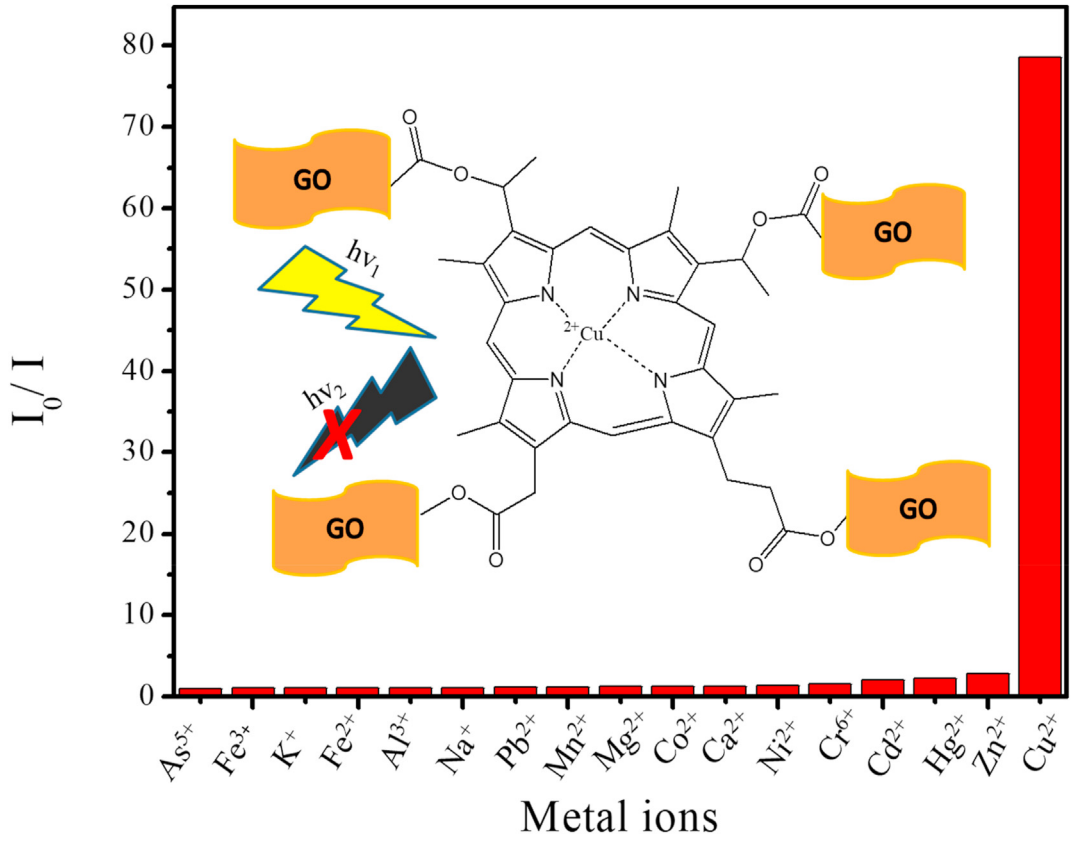

Fig. 8. Selectivity of HP-GO (10 mg L^{-1}) for different metal ions (47 μ M, I and I_0 are HP-GO fluorescence intensities in the presence and absence of Metal ions, respectively).

3.2.1. Detection of Cu^{2+} ions in real water samples using the HP-GO sensor

To evaluate the HP-GO as a sensor for Cu^{2+} in real water samples, the performance of the present sensor was determined for samples from tap water and James River water (Richmond, VA). The James River water samples were centrifuged at 9000 r.p.m for 10 min and then filtered. The resultant water samples were spiked with standard solutions containing different concentrations of

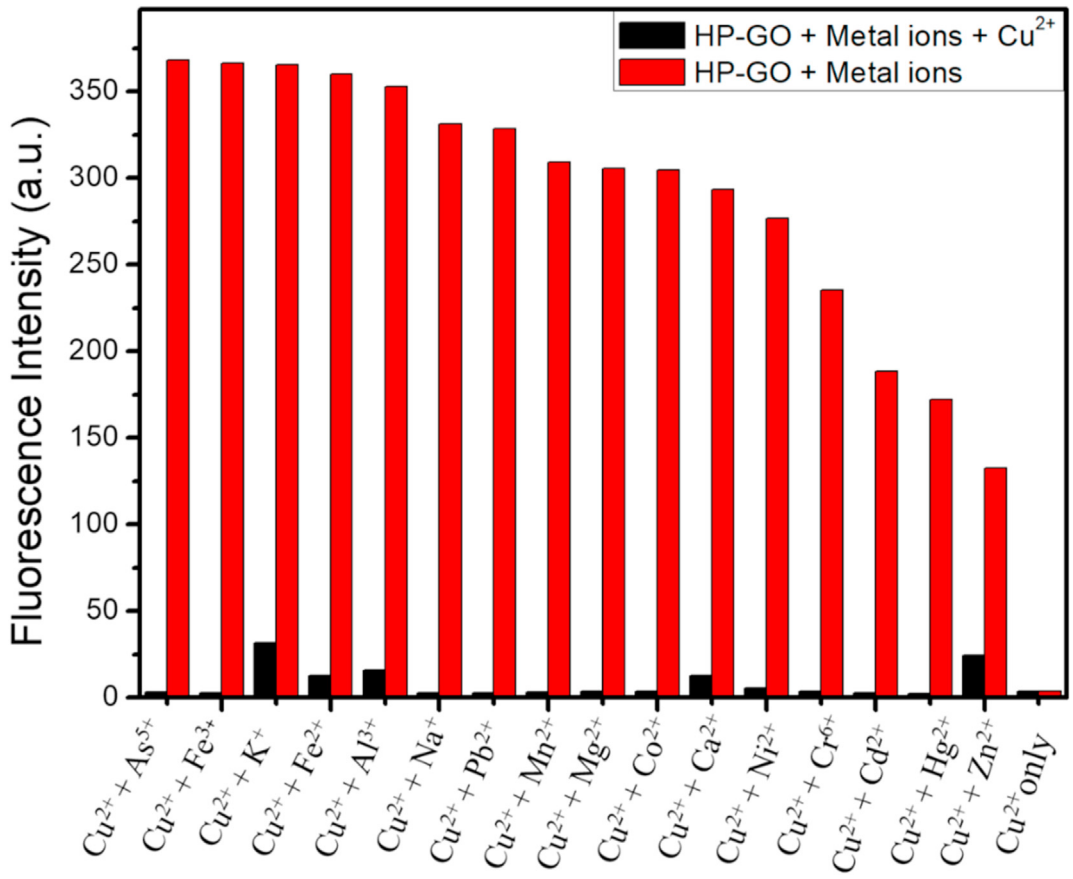

Fig. 9. Fluorescence responses of HP-GO to competing metal ions (47 μ M) redbars to Cu^{2+} ions (47 μ M, black bars), in 0.01 M phosphate buffer (pH = 8.2), HP-GO =(10 mg L^{-1}), excitation at 390 nm).

Cu^{2+}. The Cu^{2+} concentrations were measured using the fluorescence emission spectra and the linear relationship shown in Fig. 7. A shown in Table S1 (Supporting Information), the RSD for all assays are less than 0.45% and recoveries are in the range of 82.5–98.6 in spite of the interferences from various organics and minerals present in the river and tap water smaples. The HP-GO sensor still can differentiate between fresh tap or river water and that spiked with 1.5, 4.7, 6.3 μ M Cu^{2+}. These results imply that the prepared HP-GO can be used as a Cu^{2+} sensor in real environmental samples.

3.2.2. Comparison of the detection limit of the prepared HP-GO sensor towards Cu^{2+}

Table 1 lists the comparison of the detection limit of HP-GO prepared in this study with various sensors previously used for the detection of Cu^{2+}. It can be seen that the prepared HP-GO sensor have a wider linear range and good linear relation than that of the most other sensor reported in the literature, suggesting that it is considered as a promising sensor for detection of Cu^{2+} in water samples.

Table 1
Comparison of the performance of the prepared HP-GO sensor towards Cu^{2+}.

Fluorescent sensors	Performance		
	Detection limit (n M)	Linear range (n M)	Ref.
Ultrathin g-C_3N_4 nanosheets	0.5	0 - 1 × 10^4	[50]
Peptide-coated ZnS QDS	500.0	0 - 2.6 × 10^4	
c-mpg-C_3N_4	12.3	10–100	
PPNDS	1.0	0 - 5 × 10^5	
CdS QDS	100.0	–	
16-MHA capped Cds QDS	5.0	5 - 1 × 10^5	
Ligand-conjugated inorganic NPS	380.0	–	
calix [4]resorcinarene modified gold nanoparticles	100.0	—	[51]
DNA-AgNCS	500.0	0 - 3 × 10^3	[50]
Amidine/Schiff base modified polyacrylonitrile	10.0	0–100	[11]
Cyclam-Functionalized carbon dots	100.0	–	[27]
quinoline-based fluorescent sensor	135.0	–	[5]
N doped carbon dots	47.0	0 - 15 × 10^3	[25]
CdTe@SiO_2 QDs	8.4	–	[52]
Novel imidazoazine framework	100.0	–	[53]
Graphitic carbon nitride solid nanofilms	20.0	–	[26]
HP/GO nanosheets	54.0	0 - 1.18 × 10^3 3.91 × 10^3–47.27 × 10^3	This study

4. Conclusions

In summary, hematoporphyrin modified graphene oxide (HP-GO) nanosheets were prepared for highly sensitive, and selective determination of copper (II) in aqueous solution and environmental water samples. The preparation method is low cost, facile, and environmental friendly. In this method, the surface of graphene oxide is easily modified with hematoporphyrin by sulfuric acid catalyzed esterification reaction. The surface structure and morphology of the HP-GO was investigated by FTIR, XRD, UV–Vis, Raman Spectra, XPS, TEM, and Fluorescence spectra. The HP-GO exhibited excellent sensitivity for copper ions in aqueous solution, based quenching effect. Moreover, the detection limit of the HP-GO is 54 n M which is better than others reported in literature. Meanwhile, the prepared HP-GO sensor also exhibited an outstanding long-term fluorescence stability (>21days), a wide pH viable range, as well as excellent photo stability. Moreover, the prepared HP-GO sensor can also be used for detection of Cu^{2+} ions in real water samples. On the other hand, the prepared HP-GO sensor shows high anti-interference performance against 15 kinds of coexisting cations.

Associated content

Supporting Information

XPS high resolution spectra of O 1s in GO (Fig. S1). Fluorescence spectra of HP-GO under different excitation wavelength (Fig. S2). Fluorescence emission spectra of HP-GO in the presence of Cu^{2+} at different concentrations (0–3.5 ppm) (Fig. S3). Recovery of fluorescence intensity of HP-GO-Cu^{2+} using EDTA (Fig. S4). Effect of time on fluorescence quenching of HP-GO-Cu^{2+} (Figs. S5 and S6) and Selectivity of HP-GO for different metal ions (Fig. S7). Detection of Cu^{2+} ions in tap water and James river water (Table S1).

CRediT authorship contribution statement

Fathi S. Awad: prepared and characterized the samples, performed the experiments, analyzed the data, and drafted the manuscript, All the authors discussed the results and commented on the manuscript. **Khaled M. AbouZied:** contributed to the characterization of the samples. All the authors discussed the results and commented on the manuscript. **Ayyob M. Bakry:** contributed to the characterization of the samples. All the authors discussed the results and commented on the manuscript. **Weam M. Abou El-Maaty:** contributed to the characterization of the samples, All the authors discussed the results and commented on the manuscript. **Ahmad M. El-Wakil:** contributed to the characterization of the samples. All the authors discussed the results and commented on the manuscript. **M. Samy El-Shall:** conceived the project, designed the experiments, analyzed the data, and wrote the paper, All the authors discussed the results and commented on the manuscript.

Declaration of competing interest

The authors declare that they have no known competing financial interests or personal relationships that could have appeared to influence the work reported in this paper.

Acknowledgments

The authors would like to extend their gratitude to the National Science Foundation for the partial support of this work (CHE-1900094 to MSE).

Appendix A. Supplementary data

Supplementary data to this article can be found online at https://doi.org/10.1016/j.aca.2020.10.016.

References

[1] P.L. Malvankar, V.M. Shinde, Ion-pair extraction and determination of copper (II) and zinc (II) in environmental and pharmaceutical samples, Analyst 116 (1991) 1081–1084.
[2] C.N. Hancock, L.H. Stockwin, B. Han, R.D. Divelbiss, J.H. Jun, S.V. Malhotra, M.G. Hollingshead, D.L. Newton, A copper chelate of thiosemicarbazone NSC 689534 induces oxidative/ER stress and inhibits tumor growth in vitro and in vivo, Free Radic. Biol. Med. 50 (2011) 110–121.
[3] M. Wang, K.-H. Leung, S. Lin, D.S.-H. Chan, D.W. Kwong, C.-H. Leung, D.-L. Ma, A colorimetric chemosensor for Cu2+ ion detection based on an iridium (III) complex, Sci. Rep. (2014) 4.
[4] N. Singh, R.C. Mulrooney, N. Kaur, J.F. Callan, A nanoparticle based chromogenic chemosensor for the simultaneous detection of multiple analytes, Chem. Commun. (2008) 4900–4902.
[5] B. Zhang, H. Liu, F. Wu, G. Hao, Y. Chen, C. Tan, Y. Tan, Y. Jiang, A dual-response quinoline-based fluorescent sensor for the detection of Copper (II) and Iron (III) ions in aqueous medium, Sensor. Actuator. B Chem. 243 (2017) 765–774.
[6] X.-B. Zhang, J. Peng, C.-L. He, G.-L. Shen, R.-Q. Yu, A highly selective fluorescent sensor for Cu 2+ based on 2-(2′-hydroxyphenyl) benzoxazole in a poly (vinyl chloride) matrix, Anal. Chim. Acta 567 (2006) 189–195.
[7] K. Jomova, M. Valko, Advances in metal-induced oxidative stress and human disease, Toxicology 283 (2011) 65–87.
[8] H. Tapiero, D. Townsend, K. Tew, Trace elements in human physiology and pathology, Copper, Biomedicine & pharmacotherapy 57 (2003) 386–398.
[9] K.J. Barnham, C.L. Masters, A.I. Bush, Neurodegenerative diseases and oxidative stress, Nat. Rev. Drug Discov. 3 (2004) 205.
[10] N. Barnes, R. Tsivkovskii, N. Tsivkovskaia, S. Lutsenko, The copper-transporting ATPases, Menkes and Wilson disease proteins, have distinct roles in adult and developing cerebellum, J. Biol. Chem. 280 (2005) 9640–9645.
[11] I. Lee, S. Kim, S.-n. Kim, Y. Jang, J. Jang, Highly fluorescent amidine/schiff base dual-modified polyacrylonitrile nanoparticles for selective and sensitive detection of copper ions in living cells, ACS Appl. Mater. Interfaces 6 (2014) 17151–17156.
[12] D.G. Peters, J.R. Connor, M.D. Meadowcroft, The relationship between iron dyshomeostasis and amyloidogenesis in Alzheimer's disease: two sides of the same coin, Neurobiol. Dis. 81 (2015) 49–65.
[13] J.-a. Annie Ho, H.-C. Chang, W.-T. Su, DOPA-mediated reduction allows the facile synthesis of fluorescent gold nanoclusters for use as sensing probes for ferric ions, Anal. Chem. 84 (2012) 3246–3253.
[14] W.H. Organization, Life Skills Education for Children and Adolescents in Schools. Pt. 3, Training Workshops for the Development and Implementation of Life Skills Programmes, World Health Organization, 1994.
[15] N.R. Council, Copper in Drinking Water, National Academies Press, 2000.
[16] H. Ouyang, Q. Shu, W. Wang, Z. Wang, S. Yang, L. Wang, Z. Fu, An ultra-facile and label-free immunoassay strategy for detection of copper (II) utilizing chemiluminescence self-enhancement of Cu (II)-ethylenediaminetetraacetate chelate, Biosens. Bioelectron. 85 (2016) 157–163.
[17] G.P.C. Rao, K. Seshaiah, Y.K. Rao, M. Wang, Solid phase extraction of Cd, Cu, and Ni from leafy vegetables and plant leaves using amberlite XAD-2 functionalized with 2-hydroxy-acetophenone-thiosemicarbazone (HAPTSC) and determination by inductively coupled plasma atomic emission spectroscopy, J. Agric. Food Chem. 54 (2006) 2868–2872.
[18] Q. Yin, Y. Zhu, S. Ju, W. Liao, Y. Yang, Rapid determination of copper and lead in Panax notoginseng by magnetic solid-phase extraction and flame atomic absorption spectrometry, Res. Chem. Intermed. 42 (2016) 4985–4998.
[19] G. Giakisikli, P. Zachariadis, I. Kila, N. Teshima, A. Anthemidis, Flow injection solid phase extraction for trace metal determination using a chelating resin and flame atomic absorption spectrometry detection, Anal. Lett. 49 (2016) 929–942.
[20] C. Lilja, I. Betova, M. Bojinov, Electrochemical methods to study hydrogen production during interaction of copper with deoxygenated aqueous solution, Electrochim. Acta 202 (2016) 333–344.
[21] L. Ji, Q. Cheng, K. Wu, X. Yang, Cu-BTC frameworks-based electrochemical sensing platform for rapid and simple determination of Sunset yellow and Tartrazine, Sensor. Actuator. B Chem. 231 (2016) 12–17.
[22] Z. Shan, M. Lu, L. Wang, B. MacDonald, J. MacInnis, M. Mkandawire, X. Zhang, K.D. Oakes, Chloride accelerated Fenton chemistry for the ultrasensitive and selective colorimetric detection of copper, Chem. Commun. 52 (2016) 2087–2090.
[23] X. Qian, Z. Xu, Fluorescence imaging of metal ions implicated in diseases, Chem. Soc. Rev. 44 (2015) 4487–4493.
[24] X. Gao, C. Ding, A. Zhu, Y. Tian, Carbon-dot-based ratiometric fluorescent probe for imaging and biosensing of superoxide anion in live cells, Anal. Chem. 86 (2014) 7071–7078.
[25] P. Das, S. Ganguly, M. Bose, S. Mondal, A.K. Das, S. Banerjee, N.C. Das, A simplistic approach to green future with eco-friendly luminescent carbon

dots and their application to fluorescent nano-sensor 'turn-off'probe for selective sensing of copper ions, Mater. Sci. Eng. C 75 (2017) 1456–1464.
[26] H. Huang, R. Chen, J. Ma, L. Yan, Y. Zhao, Y. Wang, W. Zhang, J. Fan, X. Chen, Graphitic carbon nitride solid nanofilms for selective and recyclable sensing of Cu 2+ and Ag+ in water and serum, Chem. Commun. 50 (2014) 15415–15418.
[27] J. Chen, Y. Li, K. Lv, W. Zhong, H. Wang, Z. Wu, P. Yi, J. Jiang, Cyclam-functionalized carbon dots sensor for sensitive and selective detection of copper (II) ion and sulfide anion in aqueous media and its imaging in live cells, Sensor. Actuator. B Chem. 224 (2016) 298–306.
[28] R. Zare-Dorabei, R. Rahimi, A. Koohi, S. Zargari, Preparation and characterization of a novel tetrakis (4-hydroxyphenyl) porphyrin–graphene oxide nanocomposite and application in an optical sensor and determination of mercury ions, RSC Adv. 5 (2015) 93310–93317.
[29] H. Dong, Z. Zhao, H. Wen, Y.y.l.t.e.c. Li, F. Guo, A. Shen, F. Pilger, C. Lin, D. Shi, Poly (ethylene glycol) conjugated nano-graphene oxide for photodynamic therapy, Sci. China Chem. 53 (2010) 2265–2271.
[30] T. Poursaberi, L. Hajiagha-Babaei, M. Yousefi, S. Rouhani, M. Shamsipur, M. Kargar-Razi, A. Moghimi, H. Aghabozorg, M. Reza Ganjali, The synthesis of a new thiophene-derivative Schiff's base and its use in preparation of copper-ion selective electrodes, Electroanalysis 13 (2001) 1513.
[31] H.K. Lee, K. Song, H.R. Seo, Y.-K. Choi, S. Jeon, Lead (II)-selective electrodes based on tetrakis (2-hydroxy-1-naphthyl) porphyrins: the effect of atropisomers, Sensor. Actuator. B Chem. 99 (2004) 323–329.
[32] R. Yang, K.a. Li, K. Wang, F. Liu, N. Li, F. Zhao, Cyclodextrin-porphyrin supramolecular sensitizer for mercury (II) ion, Anal. Chim. Acta 469 (2002) 285–293.
[33] P. Kumar, Y.-B. Shim, A novel Mg (II)-selective sensor based on 5, 10, 15, 20-tetrakis (2-furyl)-21, 23-dithiaporphyrin as an electroactive material, J. Electroanal. Chem. 661 (2011) 25–30.
[34] H.M. Hassan, V. Abdelsayed, S.K. Abd El Rahman, K.M. AbouZeid, J. Terner, M.S. El-Shall, S.I. Al-Resayes, A.A. El-Azhary, Microwave synthesis of graphene sheets supporting metal nanocrystals in aqueous and organic media, J. Mater. Chem. 19 (2009) 3832–3837.
[35] S. Pourbeyram, Effective removal of heavy metals from aqueous solutions by graphene oxide–zirconium phosphate (GO–Zr-P) nanocomposite, Ind. Eng. Chem. Res. 55 (2016) 5608–5617.
[36] G. Lujanienė, S. Šemčuk, I. Kulakauskaitė, K. Mažeika, D. Valiulis, R. Juškėnas, S. Tautkus, Sorption of radionuclides and metals to graphene oxide and magnetic graphene oxide, J. Radioanal. Nucl. Chem. 307 (2016) 2267–2275.
[37] X. Guo, B. Du, Q. Wei, J. Yang, L. Hu, L. Yan, W. Xu, Synthesis of amino functionalized magnetic graphenes composite material and its application to remove Cr (VI), Pb (II), Hg (II), Cd (II) and Ni (II) from contaminated water, J. Hazard Mater. 278 (2014) 211–220.
[38] H. Maumela, R.D. Hancock, L. Carlton, J.H. Reibenspies, K.P. Wainwright, The amide oxygen as a donor group. Metal ion complexing properties of tetra-N-acetamide substituted cyclen: a crystallographic, NMR, molecular mechanics, and thermodynamic study, J. Am. Chem. Soc. 117 (1995) 6698–6707.
[39] W.S. Hummers Jr., R.E. Offeman, Preparation of graphitic oxide, J. Am. Chem. Soc. 80 (1958), 1339-1339.
[40] D.C. Marcano, D.V. Kosynkin, J.M. Berlin, A. Sinitskii, Z. Sun, A. Slesarev, L.B. Alemany, W. Lu, J.M. Tour, Improved synthesis of graphene oxide, ACS Nano 4 (2010) 4806–4814.
[41] S. Zhang, M. Zeng, W. Xu, J. Li, J. Li, J. Xu, X. Wang, Polyaniline nanorods dotted on graphene oxide nanosheets as a novel super adsorbent for Cr (VI), Dalton Trans. 42 (2013) 7854–7858.
[42] H.-L. Ma, H.-B. Zhang, Q.-H. Hu, W.-J. Li, Z.-G. Jiang, Z.-Z. Yu, A. Dasari, Functionalization and reduction of graphene oxide with p-phenylene diamine for electrically conductive and thermally stable polystyrene composites, ACS Appl. Mater. Interfaces 4 (2012) 1948–1953.
[43] T. Sreeprasad, S.M. Maliyekkal, K. Lisha, T. Pradeep, Reduced graphene oxide–metal/metal oxide composites: facile synthesis and application in water purification, J. Hazard Mater. 186 (2011) 921–931.
[44] Z. Xing, Z. Ju, Y. Zhao, J. Wan, Y. Zhu, Y. Qiang, Y. Qian, One-pot hydrothermal synthesis of Nitrogen-doped graphene as high-performance anode materials for lithium ion batteries, Sci. Rep. 6 (2016).
[45] P. Khanra, T. Kuila, N.H. Kim, S.H. Bae, D.-s. Yu, J.H. Lee, Simultaneous bifunctionalization and reduction of graphene oxide by baker's yeast, Chem. Eng. J. 183 (2012) 526–533.
[46] A. Nicolaï, P. Zhu, B.G. Sumpter, V. Meunier, Molecular dynamics simulations of graphene oxide frameworks, J. Chem. Theor. Comput. 9 (2013) 4890–4900.
[47] M.A. Habeeb Muhammed, P.K. Verma, S.K. Pal, A. Retnakumari, M. Koyakutty, S. Nair, T. Pradeep, Luminescent quantum clusters of gold in bulk by albumin-induced core etching of nanoparticles: metal ion sensing, metal-enhanced luminescence, and biolabeling, Chemistry-A European Journal 16 (2010) 10103–10112.
[48] Z. Li, L. Zhang, L. Wang, Y. Guo, L. Cai, M. Yu, L. Wei, Highly sensitive and selective fluorescent sensor for Zn 2+/Cu 2+ and new approach for sensing Cu 2+ by central metal displacement, Chem. Commun. 47 (2011) 5798–5800.
[49] Y. Hong, S. Chen, C.W.T. Leung, J.W.Y. Lam, J. Liu, N.-W. Tseng, R.T.K. Kwok, Y. Yu, Z. Wang, B.Z. Tang, Fluorogenic Zn (II) and chromogenic Fe (II) sensors based on terpyridine-substituted tetraphenylethenes with aggregation-induced emission characteristics, ACS Appl. Mater. Interfaces 3 (2011) 3411–3418.
[50] J. Tian, Q. Liu, A.M. Asiri, A.O. Al-Youbi, X. Sun, Ultrathin graphitic carbon nitride nanosheet: a highly efficient fluorosensor for rapid, ultrasensitive detection of Cu2+, Anal. Chem. 85 (2013) 5595–5599.
[51] B.A. Makwana, D.J. Vyas, K.D. Bhatt, V.K. Jain, Selective sensing of copper (II) and leucine using fluorescent turn on–off mechanism from calix [4] resorcinarene modified gold nanoparticles, Sensor. Actuator. B Chem. 240 (2017) 278–287.
[52] L. Chen, X. Tian, C. Yang, Y. Li, Z. Zhou, Y. Wang, F. Xiang, Highly selective and sensitive determination of copper ion based on a visual fluorescence method, Sensor. Actuator. B Chem. 240 (2017) 66–75.
[53] L.K. Kumawat, M. Kumar, P. Bhatt, A. Sharma, M. Asif, V.K. Gupta, An easily accessible optical chemosensor for Cu 2+ based on novel imidazoazine framework, its performance characteristics and potential applications, Sensor. Actuator. B Chem. 240 (2017) 365–375.